

FURTHER ANALYSIS OF A SNOWPACK AUGMENTATION PROGRAM  
USING LIQUID PROPANE

by

David W. Reynolds  
U.S. Department of the Interior  
Bureau of Reclamation  
Sacramento, California

Abstract. The California Department of Water Resources, with technical assistance from the Bureau of Reclamation, is continuing to pursue the use of liquid propane as a viable agent for seeding winter clouds. The tracer SF<sub>6</sub>, sulfur hexafluoride, is used to simulate the transport and dispersion of propane-generated ice crystals. Sulfur hexafluoride was released from two separate high-altitude propane dispenser sites as a proxy for seeded ice crystals. Aircraft measurements of SF<sub>6</sub> indicated that at the normal flight altitudes of 2500 m over the valley and 2680 m over the downwind ridge, the aircraft was flying near the top of the plumes. When the aircraft was able to fly below cloud base near the release altitude of 2200 m, substantial SF<sub>6</sub> was observed. A portion of the plume was observed to rise to elevations about 500 m above the release altitude. The lower portion of the plume was also observed to descend into the valley some 600 m below the release altitude. Comparison of aircraft measurements with model predictions of plume (Gaussian) horizontal dispersion compare favorably. The model verifies that the vertical dispersion of the plume is limited to only 300 to 500 m above the dispenser altitudes. Gravity waves are shown to have a significant impact on the transport of tracer/seeded crystals across the target area. The aircraft intersected 35 seeded plumes on 4 separate days. Only 11 of the 35 plumes indicated seeding effects. The lack of liquid water was considered the main reason why most plumes did not indicate seeding effects. On February 17, distinct seeding effects were noted on five of six plumes intersected from one of the sites. Apparent dynamic seeding effects were also noted on several of these passes. Precipitation at a gauge directly in line with the aircraft-observed seeding plume showed a factor of five increase in precipitation over surrounding gauges for the hour in which seeding effects would have been expected. Seeding effects were also noted on March 16, a day when the temperature at the dispenser was near or slightly above freezing.

## 1. INTRODUCTION

The LOREP (Lake Oroville Runoff Enhancement Project) is a 5-year randomized seeding experiment being conducted by the California DWR (Department of Water Resources). The long-term goal of the project is to increase runoff to Oroville Reservoir, the main reservoir of the State Water Project located in northern California. Both physical and statistical analyses are being conducted in the hope of documenting the increases in the winter snowpack obtainable by seeding winter storms with liquid propane. Reynolds (1989, 1991, 1992) describes the original design, and development and testing, of a remote propane dispenser. The present paper summarizes follow-on field studies using both aerial and ground-based tracer and microphysics observations to further document seeding efficacy using ground-based liquid propane.

During mid-January to mid-March 1993, an intensive field program was conducted within the LOREP target area, Figure 1. Emphasis was placed on documenting the transport and dispersion of a tracer and/or seeding-induced ice crystals from the dispensers to the downwind edge of the target area. Sulfur hexafluoride was released at approximately 22 kg h<sup>-1</sup> from two separate high-

altitude propane dispenser sites. Site 7 was located on the crest of the Sierra and site 9 was positioned some 5 km west of the crest. Two different locations were used to identify which site transports seeded crystals more reliably into supercooled clouds. Only limited propane seeding could be performed due to an excessively wet early winter.

Measurement systems included a highly instrumented research aircraft provided by the National Oceanic and Atmospheric Administration. A high-altitude mountaintop observatory was established within the target area (JCC in Fig. 1). The aircraft and the observatory were equipped with continuous SF<sub>6</sub> analyzers and optical ice crystal probes. The analyzer is capable of detecting SF<sub>6</sub> concentrations to 5 ppt (parts per trillion). A dual-channel radiometer was located at the mountaintop observatory to measure the integrated liquid water and vapor within passing clouds. Four time sequential syringe samplers were used to collect 15-min air samples at specified locations within the valley to monitor SF<sub>6</sub>. Locations of weighing precipitation gauges with .25-mm resolution are shown in Figure 1. In addition, three mountaintop weather stations provided measurements of supercooled liquid water through use of an icing rate meter.

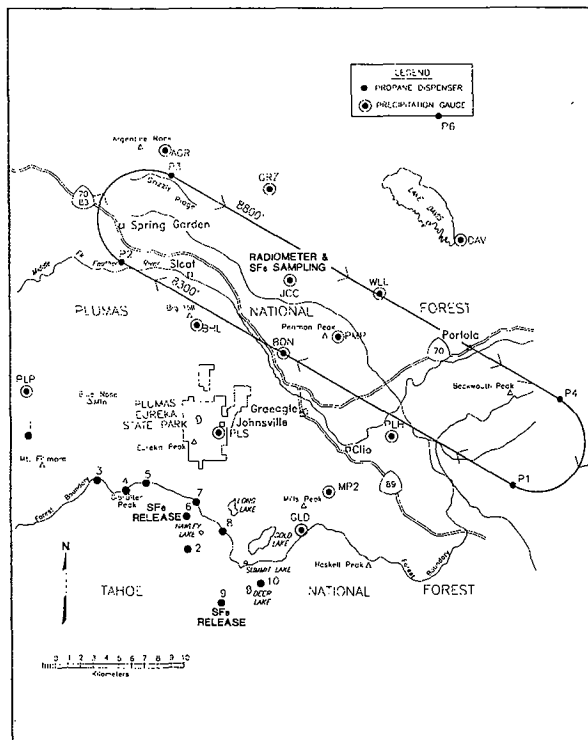


Fig. 1. Lake Oroville Runoff Enhancement Project instrumentation locations for the 1992-1993 field season. Aircraft flight tracks and way points annotated.

## 2. SULFUR HEXAFLUORIDE TRACER STUDIES

Previous tracer studies conducted for this program showed that subsidence (possibly gravity waves) to the lee of the Sierra Nevada may, at times, force some of the artificially produced ice crystals down into the valley before enough growth takes place (Reynolds, 1992). It is thus important to document the plume centerline and not just the lower portion of the plume.

The aircraft flight pattern used during research missions is shown in Figure 1. The flight leg flown between P1 and P2 was the valley track flown at 2500 m. The flight leg between P3 and P4 was the ridge track flown at 2680 m. During VFR (Visual Flight Rules) flights, these same tracks were flown but at flight levels down to 2100 m. At times the aircraft would fly short legs further downwind between P3 and P6, and from P6 to P4. During IFR (Instrument Flight Rules) conditions, these legs were flown at 2600 m.

Nine separate experiments were conducted this past season. Of these, four had both SF<sub>6</sub> and propane released, while five had SF<sub>6</sub> only.

Briefly, aircraft intersections of SF<sub>6</sub> plumes from sites 7 and 9 indicated the following. At flight altitudes of 2500 m over the valley and 2680 m over the ridge, the aircraft was generally near the tops of the SF<sub>6</sub> plume. At least half of the valley and ridge

passes found no SF<sub>6</sub> when it was expected. Plume widths over the valley averaged 3 km from site 7 (15 min downwind) and 5 km from site 9 (23 min downwind). This equates to a 3- and 3.6-m s<sup>-1</sup> horizontal dispersion for sites 7 and 9, respectively. At flight altitudes near 2200 m, plume widths increased along with SF<sub>6</sub> concentrations. This indicated the plume centerline was remaining near the release altitude. For the ridge tracks, the site 7 average plume width was 3.8 km, and the site 9 width averaged 6.6 km. At a nominal 36 min and 44 min downwind from the release, this equates to a 1.7- and 2.5-m s<sup>-1</sup> dispersion. On 1 of 3 days in which passes were made downwind of the ridge track, SF<sub>6</sub> was detected with consistency. These intersections were about 1 h downwind. Plume horizontal dimensions of 14 and 15 km were observed for sites 7 and 9, respectively, equating to a 4-m s<sup>-1</sup> spread rate. In general, the plume from site 9, initiated further west from the crest, experienced more horizontal and vertical dispersion and thus appears to be a better location for releasing seeding material.

### 2.1 GUIDE Model Verification

The GUIDE model is a simple two-dimensional kinematic model incorporating Gaussian plume dispersion (Raubert et al., 1988). The model is used operationally to predict the area of effect from seeding. The model has 5-km horizontal resolution and 100-m vertical resolution. Horizontal winds are derived by simply extrapolating winds measured from the Johnsville rawinsonde (Fig. 1). Vertical motions are derived by multiplying the component of the wind normal to the model terrain by the slope of the terrain between model grid points. This method of calculating vertical velocities generally overestimates the magnitude of the vertical motions, in the absence of gravity waves. It will be shown later that gravity waves are frequently present over the target area.

For each of the 9 days having SF<sub>6</sub> releases and aircraft sampling, the model was initialized using the sounding closest in time to the release. This was within 1 h of release time. The model-predicted plume was plotted over the target area topography. An example of this is described below.

On March 9, detailed vertical and horizontal measurements of plumes from both sites were documented in VFR conditions. Figure 2 shows the predicted plumes (dotted lines) from both sites based on the 0900 PST Johnsville sounding. Aircraft-observed SF<sub>6</sub> concentrations above 10 ppt are noted by symbols. [Box, 10-15 ppt; plus, 15-50 ppt; X, 50-100 ppt; asterisk, 100-150 ppt; shaded star, 150-200 ppt; sun, 200-250 ppt; open star, >250 ppt]. The maximum concentration observed was over 300 ppt. The predicted plumes are in line with observed SF<sub>6</sub> intersections over the valley. However, over the ridge, the tracer is to the right of the predicted plumes. This indicates that the plumes may be going around the highest terrain to the right. Average aircraft wind directions measured over the ridge were 5 to 8 degrees more westerly than observed over the valley.

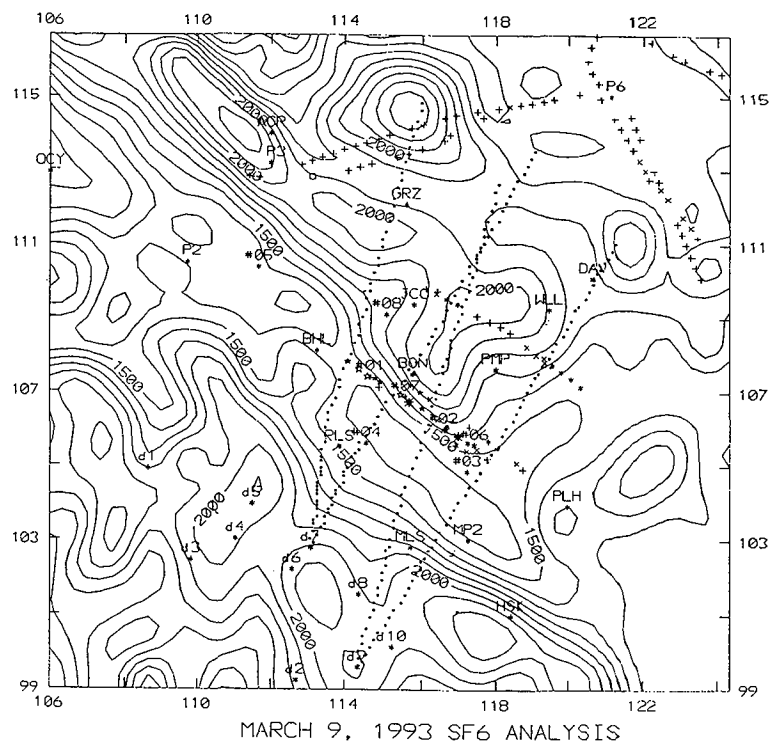


Fig. 2. GUIDE-model-predicted plumes (dotted lines) from sites 7 and 9 overlaid onto terrain contours for 9 March, 0900 PST. Aircraft-observed  $\text{SF}_6$  concentrations above 10 ppt noted by symbols.

Downwind of the ridge, the observed plumes are wider than model predictions. Substantial mixing downwind of the second ridge is causing rapid diffusion of the plumes. A vertical cross section of  $\text{SF}_6$  concentrations for March 9 is shown in Figure 3. The plume centerline appears to be moving almost horizontally over the valley, then displaced vertically a few hundred meters over the second ridge. Some  $\text{SF}_6$  was observed in the valley and at JCC. The discussion in Section 2.2 is relevant to this observation.

Of the nine experiments conducted with aircraft sampling of  $\text{SF}_6$ , all but one had model-predicted horizontal plume locations within 1 to 2 km of observed locations. The model-predicted vertical plume displacement is usually within a few hundred meters of the maximum height of plume rise.

## 2.2 Influence of Gravity Waves on the Transport of Seeding Material

It is well known that downwind of the Sierra crest, mountain lee waves are observed during stable atmospheric conditions (Holmboe and Klieforth, 1957). It has also been shown that the ascent rate of rawinsonde balloons can be used to identify the presence of these lee waves (gravity waves) (Lalas and Einaudi, 1980, Reid, 1972, and Shutts et al., 1993). These authors show that the ascent rate can be measured to within  $.2 \text{ m s}^{-1}$  using 20- to 40-s pressure increments. The data from the Johnsville rawinsonde are recorded every 2 s and the ascent

rate can be calculated every 20 s. Based on the free lift of the balloon and the payload, a nominal ascent rate of  $5 \text{ m s}^{-1}$  is assumed. This was subtracted from the observed ascent rate to estimate free air vertical velocity. This was then plotted with respect to distance from Johnsville to observe any trends in vertical motions. An example of this is shown in Figure 4 for the March 9 case. A generalized streamline analysis is shown based on the computed vertical velocities and approximating a single lee wave. This lee wave motion is obviously restricting the vertical transport of the tracer until the air traverses almost completely past the valley. The tracer is then transported vertically up and over the second ridge. The aircraft sampling locations for March 9 are shown to be in a location where the tracer would be transported to these sampling levels. If seeding had occurred on this day, little growth would have occurred during downward transport. Subsequent growth on the windward side of the second ridge may not be fast enough to allow the crystals to fall out before being transported over the gauge network.

Analysis of soundings taken during  $\text{SF}_6$  releases both this year and from previous years indicates that this lee wave is almost always present. It is the reason why at least some  $\text{SF}_6$  has been observed in the valley in 23 of 25 tracer experiments conducted. The amplitude and phase of the wave varies considerably. In certain cases, it can rapidly transport the tracer down into the valley. In other cases, it can rapidly transport the tracer/crystals upward over

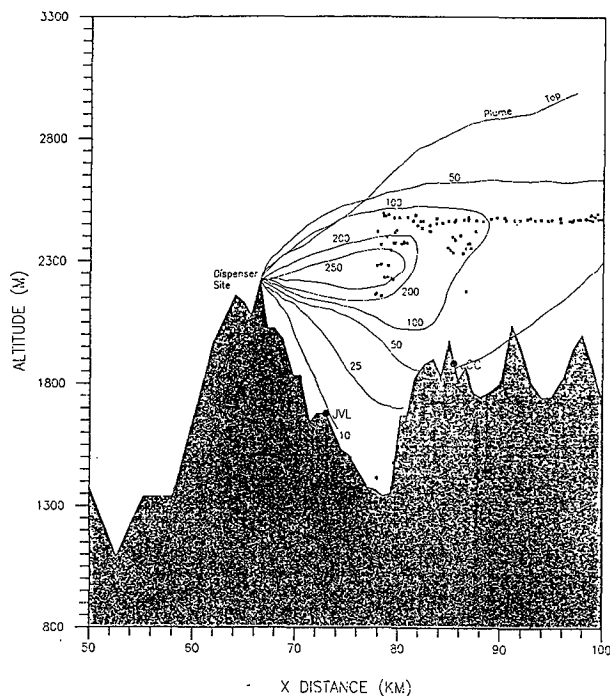


Fig. 3. Cross section from Sierra Crest to Grizzly Ridge showing contoured  $\text{SF}_6$  concentrations observed by aircraft and ground based sequential samplers for 9 March. Asterisks denote sampling locations. Model-predicted plume top shown.

the center of the valley and well over the second ridge.

In an attempt to better document this lee wave and its effects on vertical transports, a 915-MHz wind profiler (Rodgers et al., 1993) was installed this winter near Graeagle (see Fig. 1). A statistical consensus of profiler winds is produced each hour. Ground clutter can seriously affect these winds in the absence of precipitation. Figure 5 shows a comparison of profiler 1-h consensus winds compared to the instantaneous winds from the rawinsonde for February 10, 1994, at 1700 GMT. The profiler vertical velocities shown are overwhelmed by particle fall speeds in this example. This day is fairly typical in showing that the profiler winds and rawinsonde winds agree quite well. It is assumed that the profiler is about a quarter to half wavelength further downwind than JVL and thus in the bottom or rising portion of the wave. Notice in the descending air experienced by the balloon near the crest (2200 m) and in the rising air between 2500 and 4000 m the profiler winds underestimate the rawinsonde-measured wind speeds. This may indicate the variable nature of the wave during 1 h.

The profiler-observed vertical velocities do not indicate the strong rising motion observed by the balloon from 2500 m to 4000 m, even though the balloon passed within the sampling volume of the profiler. This may indicate particle fall speeds are cancelling out the free air vertical motions. An analysis of the profiler spectra may help address this question.

Figure 6 shows the vertical motions calculated from the GUIDE model for February 10, using the 1700 GMT sounding. Although crude, it does simulate the general trend observed from the balloon ascent rates. A more detailed three-dimensional, nonhydrostatic model is needed to better predict the phase and amplitude of the wave and its relationship to stability, wind speed, and wind direction.

### 2.3 Direct Detection of Seeding Effects

Of the 4 days having both  $\text{SF}_6$  and propane releases, February 17 provided the best documented case of seeding effects. On February 17, seeding was conducted ( $13 \text{ L h}^{-1}$  propane) from site 7 from 0830 to 0930 PST and from site 9 from 0930 to 1030 PST. Temperatures at the dispensers were near  $-5^\circ \text{C}$ . Radiometric liquid water averaged .1 mm. Mountaintop icing data showed liquid water contents of  $.1 \text{ g m}^{-3}$ .

Of the eight aircraft intersections of the site 7  $\text{SF}_6$  plume (four valley and four ridge), no definitive seeding effects were observed. Data from both aircraft liquid water probes indicated liquid water contents averaged less than  $.02 \text{ g m}^{-3}$  and cloud droplet concentrations averaged less than 25 per cc within the eight plumes.

The plume from site 9 was intersected six times (three valley and three ridge). Four had distinct seeding signatures. An increase in cloud water was noted within site 9 plumes. Pass 13, along the valley, shows the most distinct seeding signature observed. Figure 7 shows a well defined  $\text{SF}_6$  plume (vertical lines denote 11-s lag) centered on a region of enhanced, but rather small ice crystals (dashed line in 2D panel are crystals  $< 250$  microns). A distinct habit change from hexagonal to needle crystals occurred at this location. The liquid water at this location is also the highest observed on this flight. This is contradictory to the glaciogenic seeding hypothesis in that seeding should reduce cloud water by growth of the enhanced ice crystals. An explanation is that seeding rates with propane are much higher than normally used for silver iodide,  $6000 \text{ g h}^{-1}$  vs  $30 \text{ g h}^{-1}$ , respectively. Because of homogenous nucleation, propane produces very rapid condensation and subsequent freezing of billions of ice crystals releasing latent heat which can increase the clouds buoyancy by several tenths of degrees centigrade. These results are consistent with numerical model results simulating seeding of orographic clouds (Orville et al., 1984). Similar, but not as impressive signatures were seen on the other three passes. One pass on February 9 indicated results very similar to this case.

One minute averages (about 4.8 km of flight) of crystal concentrations and calculated precipitation rates within and outside the site 9 seeding plumes showed a 33% increase in ice crystal concentrations and an 18% increase in calculated precipitation rate.

The tracer  $\text{SF}_6$  was on a trajectory passing over the Jackson Creek Observatory (JCC) and directed at the GRZ gauge. The  $\text{SF}_6$  sequential

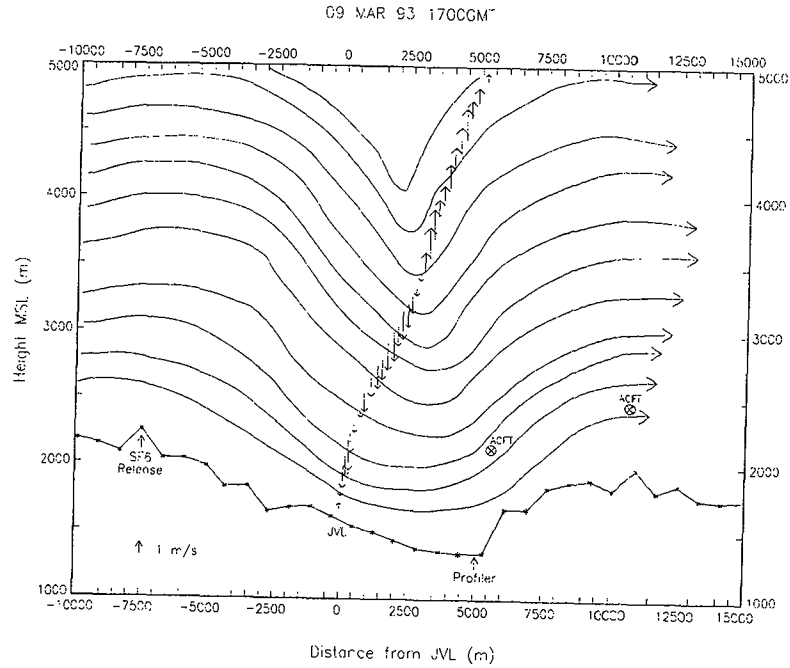


Fig. 4. Cross section of terrain relief along 205 degrees with the balloon-observed free air vertical velocities denoted by up or down arrows. The magnitude of the vertical velocity is scaled by arrow length. The location of aircraft sampling, SF<sub>6</sub> release, and the location of the wind profiler used in 1994 are shown.

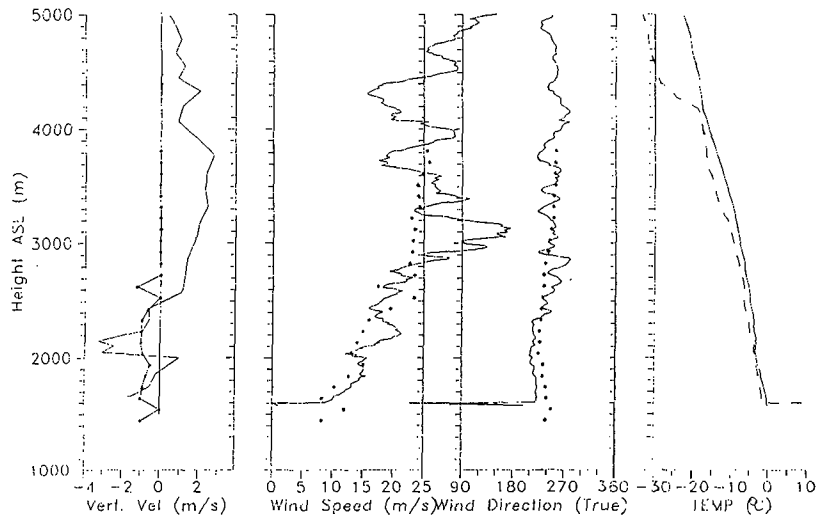


Fig. 5. Comparison of rawinsonde-observed horizontal and vertical winds (solid line) and profiler 1-h consensus winds (asterisks) for February 10, 1994. The rawinsonde-measured temperature and dewpoint vertical profiles are also shown.

3400.	.68	.68	.68	-2.03	1.69	1.02	.34	-1.02	.34	-.68	.34	.6
3300.	.89	.89	.89	-2.68	2.24	1.34	.45	-1.34	.45	-.89	.45	.8
3200.	1.11	1.11	1.11	-3.34	2.78	1.67	.56	-1.67	.56	-1.11	.56	1.1
3100.	1.19	1.19	1.19	-3.56	2.96	1.78	.59	-1.78	.59	-1.19	.59	1.1
3000.	1.44	1.44	1.44	-4.33	3.61	2.17	.72	-2.17	.72	-1.44	.72	1.4
2900.	1.56	1.56	1.56	-4.68	3.90	2.34	.78	-2.34	.78	-1.56	.78	1.5
2800.	1.45	1.45	1.45	-4.35	3.63	2.18	.73	-2.18	.73	-1.45	.73	1.4
2700.	1.17	1.17	1.17	-3.50	2.91	1.75	.58	-1.75	.58	-1.17	.58	1.1
2600.	1.02	1.02	1.02	-3.05	2.54	1.52	.51	-1.52	.51	-1.02	.51	1.0
2500.	.82	.82	.82	-2.45	2.04	1.23	.41	-1.23	.41	-.82	.41	.8
2400.	.59	.59	.59	-1.76	1.47	.88	.29	-.88	.29	-.59	.29	.5
2300.	.63	.63	.63	-1.88	1.57	.94	.31	-.94	.31	-.63	.31	.6
2200.	.71	.71	.71	-2.12	1.76	1.06	.35	-1.06	.35	-.71	.35	.7
2100.	.74	.74	.74	-2.21	1.84	1.10	.37	-1.10	.37	-.74	.37	.7
2000.	.65	.65	.65	-1.95	1.62	1.04	.32	-1.04	.32	-.65	.32	.65
1900.	.53	.53	.53	-1.59	1.32	.94	.26	-.94	.26	-.53	.26	.53
1800.	.41	.41	.41	-1.14	.95	.81	.20	-.81	.20	-.41	.20	.41
1700.	.29	.29	.29	-.69	.56	.68	.14	-.68	.14	-.29	.14	.29
1600.	.17	.17	.17	-.24	.17	.55	.08	-.55	.08	-.17	.08	.17
1500.	.05	.05	.05	.00	.00	.44	.02	-.44	.02	-.05	.02	.05
1400.	.00	.00	.00	.00	.00	.33	.00	-.33	.00	-.00	.00	.00
1300.	.00	.00	.00	.00	.00	.22	.00	-.22	.00	-.00	.00	.00
1200.	.00	.00	.00	.00	.00	.11	.00	-.11	.00	-.00	.00	.00

Fig. 6. GUIDE-model-calculated vertical velocities over the project terrain (asterisks). Horizontal grid spacing is 5 km. Vertical grid spacing is 100 meters. These data should be compared to the rawinsonde-observed vertical velocities shown in Figures 4 and 5. Vertical velocities need to be considered only up to 2800 m since SF<sub>6</sub> is almost always observed below this altitude.

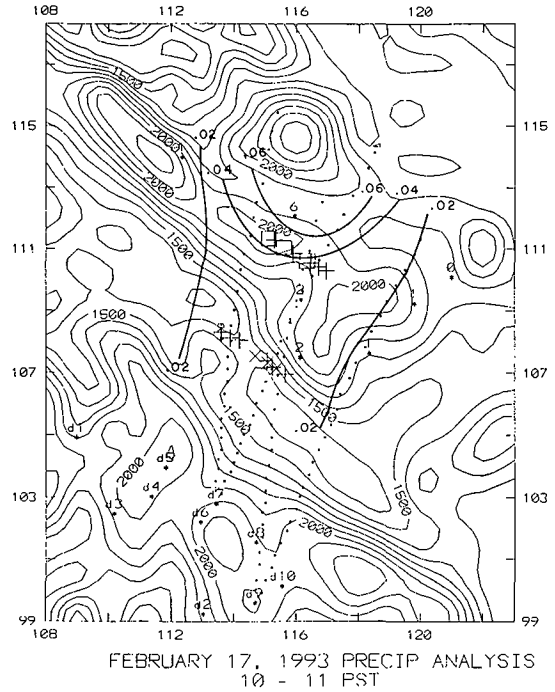


Fig. 8. Isohyets for 1000 to 1100 PST 17 February with aircraft-observed SF<sub>6</sub> locations and GUIDE model plumes noted.

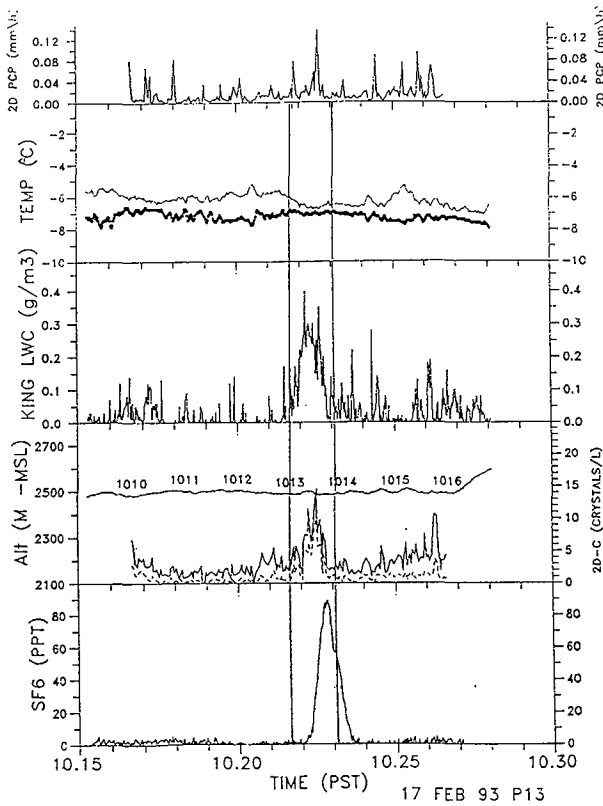


Fig. 7: Variables observed or calculated from aircraft observations during plume tracing experiment of February 17. From top to bottom: calculated precipitation rate from 2D ice probe; temperature (thin) and dew point (heavy); cloud liquid water; cloud ice concentration (solid) and particles classified as tiny (dashed); SF<sub>6</sub> concentration. Vertical lines denote true position of SF<sub>6</sub> plume accounting for 11 s lag.

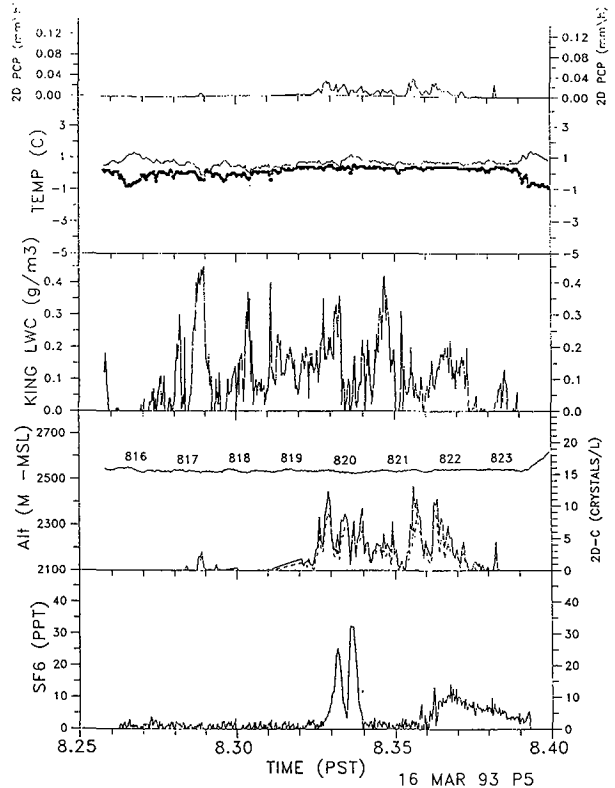


Fig. 9. Same as Fig. 7 but for 16 March pass 5 along valley track. Site 9 then site 7 plumes sampled.

sampler, about a kilometer west of JCC, indicated SF<sub>6</sub> from both site 7 (0930 to 1000 PST) and site 9 releases (1015 to 1045 PST). There were indications of ice crystal concentration increases on the 2D probe at JCC during the period from 0900 to 1015 PST of up to 30 L<sup>-1</sup> above a background of 15 L<sup>-1</sup>. Precipitation increases were also noted for those gauges within the fallout trajectory. Figure 8 is an isohyetal map of 1-h precipitation totals in the gauge network between 1000 and 1100 PST. Here we see more precipitation in the gauge at GRZ (.06 in), directly in line with the tracer trajectory.

March 16 provided documentation of seeding effects when ambient air temperatures were near 0 °C. Seeding was conducted for 1 h from both sites 7 and 9. Aircraft observations showed temperatures just above freezing at 2500 m. Liquid water contents were near the highest observed on any flight. Of the five SF<sub>6</sub> plumes observed by aircraft from site 7, three indicated apparent seeding effects. This is notable in that seeding was performed near 0 °C.

Figure 9 shows the aircraft data for pass 5 along the valley. The site 9 plume is intersected first at 0820 PST followed by site 7 at 0822 PST. Liquid water is observed along the entire pass. The ice crystal probe detects ice crystals near and during plume intersections. Almost all crystals are less than 250 microns (dotted line). Images (not shown) indicated the crystals to be hexagonal plates, consistent with fog seeding done near 0 °C with dry ice (Deshler et al., 1987). It has been observed that propane seeding in fog at temperatures near +1 to +2 °C has caused precipitation (Gerdel, 1968). Gerdel suggests that a propane hydrate or clathrate is formed by the inclusion of gas molecules in the ice crystal. Such crystals have a melting, or dissociation, between +1 and +6 °C. This is dependent on the number of molecules of propane included in the clathrate. It is clear that more study is needed to verify this hypothesis.

### 3. CONCLUSIONS

Aircraft measurements of SF<sub>6</sub> released from two separate high-altitude propane dispenser sites indicate the plumes rarely rise above 2700 m or 500 m above the release altitude. Comparison of aircraft measurements with GUIDE model predictions of plume horizontal and vertical dispersion compare favorably. However, it is apparent that commonly observed lee waves have a significant impact on the transport of seeded crystals over the target area.

The aircraft intersected 35 seeded plumes on four separate days. Only 11 of the 35 plumes indicated seeding effects. The lack of liquid water minimized seeding effects. On February 17, distinct seeding effects were noted on five of six plumes intersected from one of the sites. Apparent dynamic seeding effects were noted on several of these passes. Precipitation at a gauge directly in line with the aircraft-observed seeding plume showed a factor of five increase in precipitation over surrounding gauges. Seeding effects using liquid propane were noted 1 day when the temperature at the dispenser was near or slightly above freezing.

**Acknowledgements.** The LOREP is managed by the California Department of Water Resources and funded by the State Water Project. The Bureau of Reclamation provided technical direction.

### 4. REFERENCES

- Benner, R.L., and R. Lamb, 1985: A fast response continuous analyzer for halogenated atmospheric tracers. *J. Atmos. and Ocean. Tech.*, **2**, 582-589.
- Deshler, T., D.W. Reynolds and J.H. Humphries, 1987: Observations of snow crystal concentration, habit, riming and aggregation collected at the ground during six fog seeding experiments. *Proc. 11th Conf. Wea. Modif.*, Edmonton, Canada, Amer. Meteor. Soc., 118-121.
- Gerdel, R.W., 1968: Note on the use of liquified propane for fog dispersal at the Medford-Jackson Airport, Oregon. *J. Appl. Meteor.*, **7**, 1039-1040.
- Holmboe, J., and H. Klieforth, 1957: Investigations of Mountain Lee Waves and the Air Flow Over the Sierra Nevada. Final Report, Contract No. AF19(604)-728, Dept. of Meteor., UCLA. 299 pp.
- Lalas, D.P., and F. Einuadi, 1980: Tropospheric gravity waves: their detection by and influence on rawinsonde balloon data. *Quart. J. R. Meteor. Soc.*, **106**, 885-864.
- Orville, H.D., R.D. Farley and J.H. Hirsch, 1984: Some surprising results from simulated seeding of stratiform-type clouds. *J. Climate Appl. Meteor.*, **23**, 1585-1600.
- Rauber, R.M., R.D. Elliott, J.O. Rhea, A.W. Huggins and D.W. Reynolds, 1988: A diagnostic technique for targeting during airborne seeding experiments in wintertime storms over the Sierra Nevada. *J. Appl. Meteor.*, **27**, 811-828.
- Reid, S.J., 1972: An observational study of lee waves using radiosonde data. *Tellus*, **24**, 93-596.
- Reynolds, D.W., 1989: Design of a ground based snowpack enhancement program using liquid propane. *J. Wea. Mod.*, **21**, 29-34.
- Reynolds, D.W., 1991: Design and field testing of a remote liquid propane dispenser. *J. Wea. Mod.*, **23**, 49-53.
- Reynolds, D.W., 1992: A snowpack augmentation program using liquid propane. Preprints, AMS Symposium on Planned and Inadvertent Weather Modification. Atlanta, GA. 88-95.
- Rodgers, R.R., W.L. Ecklund, D.A. Carter, K.S. Gage and S.A. Ethier, 1993: Research applications of a boundary-layer wind profiler. *Bull. A. M. S.*, **74**, 567-580.
- Shutts, G.J., P. Healy and S.D. Mobbs, 1993: A multiple sounding technique for the study of gravity waves. *Quart. J. R. Meteor. Soc.*, **120**, 59-77.